Food Chemistry 514 (2026) 148889

Contents lists available at ScienceDirect

Food Chemistry

journal homepage: www.elsevier.com/locate/foodchem

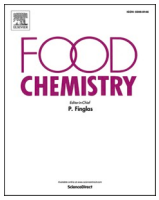

Development and methodological user-validation in industry of a 3D-printed biosensing toolkit for tropane alkaloid detection

Ids B. Lemmink [a,b,1,*], Eleonora Rollo [c,d,1], Erik Beij [b], Anne-Catherine Huet [e], Toine F.H. Bovee [b], Michele Suman [c,d,*], Gert IJ. Salentijn [a,b,*]

[a] Laboratory of Organic Chemistry, Wageningen University & Research, Stippeneng 4, 6708, WE, Wageningen, the Netherlands
[b] Wageningen Food Safety Research, Wageningen University & Research, Akkermaalsbos 2, 6708, WB, Wageningen, the Netherlands
[c] Barilla G. e R. Fratelli S.p.A., Analytical Food Science, Via Mantova, 166, 43122, Parma, Italy
[d] University of Parma, Department of Food and Drug, Viale delle Scienze 27, A-43124, Parma, Italy
[e] CER Groupe, Rue du Point du Jour, 8, 6900 Marloie, Belgium

ARTICLE INFO

Keywords:
User-validation
Immunoassay
3D-printing
Tropane alkaloids
Food safety

ABSTRACT

The number of biosensors for food contaminants are growing, yet few are tested in real-world settings. Here, we developed and validated a biosensor for detecting tropane alkaloids in buckwheat, emphasizing in-field accuracy and user-experience. Sixty participants from a major food producer tested the biosensor in a pre-structured manner. All quality control employees (n = 31) correctly identified blank or contaminated buckwheat. However, non-analytical-users (n = 29) showed lower accuracy when visually interpreting icLFIA-results (Kappa-score = 0.5/1), which improved substantially when using a digital reader (Kappa-score = 0.9/1). Post-test questionnaires yielded an excellent usability score (88/100 ± 8). A difficulty score, based on how many participants struggled and the corresponding perceived difficulty, allowed identification of challenging workflow steps. Notably, most challenging steps could be resolved by adjusting the instructions. This user-validation represents a pioneering effort in food safety analysis, especially point-of-need detection, to offer quantitative evidence for claims related to stakeholder usability and provides a framework for other innovative (bio)sensing approaches.

1. Introduction

A range of drivers, such as climate change, green transition, and geopolitics affect the risk of food contaminations (e.g. with natural toxins), reinforcing the need for the food industry to adapt to these realities in their product safety assessment (Lemmink, Straub, et al., 2024; Rockström et al., 2020; Zurek et al., 2022). In response, a growing number of point-of-need tools are being developed for rapid and cost-effective screening of such contaminants (Lemmink, Straub, et al., 2024). These devices are designed to enable end-users, such as food safety inspectors and quality control (QC) personnel, to perform fast, qualitative screening directly at the point-of-need (Lemmink et al., 2025). Although many point-of-need tools have been developed, only a few have undergone a validation to determine their analytical performance (Geballa-Koukoula et al., 2023; Ross et al., 2023). Even more critically, point-of-need tests that are validated are often evaluated only by (i) scientists in (ii) controlled laboratory settings, rather than by (i) the intended end-users in (ii) real-world settings (e.g., slaughterhouses, silos, or food production facilities) (Geballa-Koukoula et al., 2023; Ross et al., 2023). This disconnect presents a major hurdle towards understanding the performance of these tools during actual use.

A screening method for food safety should in principle be validated in a laboratory to demonstrate that, when properly used under specific conditions, the uncertainty associated with the outcome is within the internationally accepted criteria for enforcement purposes. For example, for plant toxins (such as atropine and scopolamine), screening methods should be validated to be fit-for-purpose by analyzing at least 20 blank and contaminated samples in the food commodity of interest. After the samples are measured, a cut-off value with an estimated FN-rate of 5% should be established and the corresponding estimated false positive (FP) rate reported (EU regulation 2023/2783) (European Commission, 2023).

* Corresponding authors.
E-mail addresses: ids.lemmink@wur.nl (I.B. Lemmink), michele.suman@barilla.com (M. Suman), gert.salentijn@wur.nl (G.IJ. Salentijn).
[1] Shared first authors that contributed equally to this manuscript.

https://doi.org/10.1016/j.foodchem.2026.148889
Received 31 August 2025; Received in revised form 11 February 2026; Accepted 12 March 2026
Available online 21 March 2026

Still, a conventional laboratory validation does not account for uncertainty associated with taking the test out of the lab and to the point-of-need. Moreover, critical assessment of the usability and in-field accuracy of such tests is not provided. Often, the starting point for point-of-need testing is based on the World Health Organization (WHO) Real-time connectivity, Ease of specimen collection, Affordable, Sensitive, Specific, User-friendly, Rapid & Robust, Equipment-free, and Deliverable to end-users (REASSURED) criteria (Mabey et al., 2004). While it is typically accepted that most screening tests are or can be cost-effective, the user-experience of these tests are mostly not evaluated, and instead assumed as 'REASSURED by design' – which is not necessarily reassuring (Geballa-Koukoula et al., 2023; Lattanzio et al., 2013; Lemmink, Straub, et al., 2024). User-experience is defined by ISO (9241–11) as "A person's perceptions and responses that result from the use and/or anticipated use of a product, system or service" (Grassi et al., 2017). User-experience is generally considered as an holistic extension of usability in which the interactions of the end-user with the tool before, during, and after use are included (Rusu et al., 2015). Several health-monitoring tests have been assessed on their user-experience during a user-validation (Grym et al., 2019; Jing et al., 2022; Ng et al., 2012; Yonel et al., 2022; Young et al., 2019). In an elaborate user-validation of a SARS-CoV-2 test, the user-experience was assessed on five different criteria's: i) ease-of-use, ii) effectiveness, iii) efficiency, iv) accuracy, and v) satisfaction (Jing et al., 2022). Although health-monitoring and food safety tests are both focused on rapid analysis, food safety tests generally require a more elaborate sample preparation workflow. This typically includes extraction, analyte enrichment, and matrix clean-up steps, due to the high complexity, solidity, and heterogeneity of many food products (Lemmink, Straub, et al., 2024). During such sample preparation, the main challenge is that the presence of matrix should be minimized while still extracting and preferably concentrating the analytes-of-interest.

In previous work, we have successfully developed and validated strategies for the point-of-need detection of tropane alkaloids, which are strictly regulated poisonous plant toxins that may contaminate grains through mechanical co-harvesting of toxin-producing weeds (Gravador et al., 2024; Lemmink et al., 2024). Since the tropane alkaloids atropine and scopolamine must not exceed 10 μg kg^{-1} in cereals (EU regulation 2023/915), it is critical for both food safety authorities and food producers to be able to monitor their ingredients and products effectively and efficiently. This was the reason that the fast tests were developed in the first place. In this work, we challenged the assumption underlying the previous laboratory test development and validation, and performed a quantitative investigation of the in-field accuracy and user-experience through a methodological user-validation. The primary objective was to develop a broadly applicable framework for generating evidence to support claims regarding ease-of-use and practical applicability of (bio) sensing technologies at the point-of-need. Prior to the user-validation, we hypothesized that: (i) when expert end-users analyze blank or highly contaminated buckwheat samples, errors will arise more frequently from complex sample handling than from interpretation of the icLFIA results, (ii) automated icLFIA read-out will be more accurate then visual read-out, and (iii) end-users with at least moderate laboratory-experience will interpret icLFIA results more accurately than end-users without such background. In addition, as a secondary objective, we aimed to identify which steps in the sample-handling workflow caused difficulties, to understand why these difficulties occurred, and to propose potential solutions, highlighting the importance of iterative improvements.

2. Materials and methods

2.1. Experimental strategy

A 3D-printed biosensing toolkit for tropane alkaloid detection in buckwheat cereals was evaluated through an elaborate user-validation at a major food producing company. The overall workflow of this research is summarized in Fig. 1. First, the previously developed and validated modular workflow for atropine detection was integrated in a 3D-printed biosensing toolkit, aiming to enhance user-friendliness by reducing the number of handling steps and providing structure to the test kit (see Fig. 1I) (Lemmink et al., 2024). Then, the biosensing toolkit was tested by 60 employees of Barilla company across several QC-laboratories in Italy (see Fig. 1II). During this user-validation, the biosensing toolkit was assessed based on its in-field accuracy and user-experience. The in-field accuracy was assessed based on the test results and the interpretation of those results by the end-users, while user-experience was measured through post-test questionnaires. Based on the feedback received during the user-validation, a rapid icLFIA was developed to allow for the rapid monitoring of scopolamine with the biosensing toolkit (see Fig. 1III).

2.2. Chemicals and consumables

2.2.1. Chemicals

Scopolamine (>99%), tropine (97%), homatropine hydrobromide (>99%), aposcopolamine (>99%), atropine (>99%), and butyl acetate (>99%) were purchased from TCI Europe (Zwijndrecht, Belgium) and formic acid (FA, LC-MS grade), Tween 20, and bovine serum albumin (BSA, ≥98%) from Sigma Aldrich Co. (Saint Louis, USA). Anisodamine (>98%), and anisodine hydrobromide (>99%) were purchased from Phytolab (Vestenbergsgreuth, Germany). Methanol (MeOH, LC-MS grade) and acetonitrile (ACN, LC-MS grade) were obtained from Actu-all Chemicals (Oss, The Netherlands) and sodium hydroxide (NaOH, pellets), and phosphate-buffered saline (PBS) tablets from Merck KGaA (Darmstadt, Germany). 'Spezial Schwartz 4' carbon nanoparticles were purchased from Degussa AG (Frankfurt, Germany) and goat anti-mouse IgG in PBS (pH 7.6) (1.2 mg mL^{-1}; AffiniPure F(ab')2 Fragment GAM IgG Fcγ) from Jackson Immunoresearch Laboratories Inc. (West Grove, USA). A monoclonal atropine-specific antibody and an atropine-BSA conjugate were obtained from Jiangnan University (Wuxi, China). A polyclonal anti-scopolamine antibody was obtained from CER Groupe (Marloie, Belgium) (Mulder et al., 2014). Deionized water was obtained from a Milli-Q direct ultrapure water system (Millipore, USA). The running buffer (RB) for the icLFIAs as applied in this work was 0.01 M PBS in water containing 1% BSA and 0.05% Tween 20. PLA+ filament (diameter = 1.75 mm) was obtained from 123-3D.nl (Almere, The Netherlands), and proprietary clear resin Type V4 from Formlabs (Summerville, USA).

2.2.2. Consumables

UniSart 95 CN nitrocellulose membranes were purchased from Sartorius (Gottinghem, Germany) and 30-mL plastic vials from Dakla-Pack Europe (Lelystad, The Netherlands). Plastic backing cards (30 cm × 6 cm), glass fiber (25.4 cm × 30.48 cm), and sample pads (21 cm × 29.7 cm) were obtained from Kenosha (Amstelveen, The Netherlands) and Whatman 1 CHR chromatography paper (200 mm × 200 mm) from Sigma-Aldrich corporation (Saint Louis, USA). Protein LoBind safe-lock tubes 1.5-mL and 2.0-mL (PCR clean) were purchased from Eppendorf Corporate (Hamburg, Germany). Plastic stopcock valves were purchased from Nanjing life store (Nanjing, China) and ceramic homogenizers from Thermo Fisher scientific (Hampton, USA).

2.2.3. Preparation of (user-)validation samples

Due to the route of contamination (i.e., by cross-crop contamination), certified reference materials for tropane alkaloids are not commercially available. As a result, most analytical methods have been validated using materials spiked in-house (Dzuman et al., 2020; Gonçalves et al., 2020; Marín-Sáez et al., 2019; Rausch et al., 2021; Veršilovskis et al., 2020). In this study, milled buckwheat cereals were purchased from local grocery stores. Buckwheat was selected as food commodity of interest as it has been reported to be relatively frequently

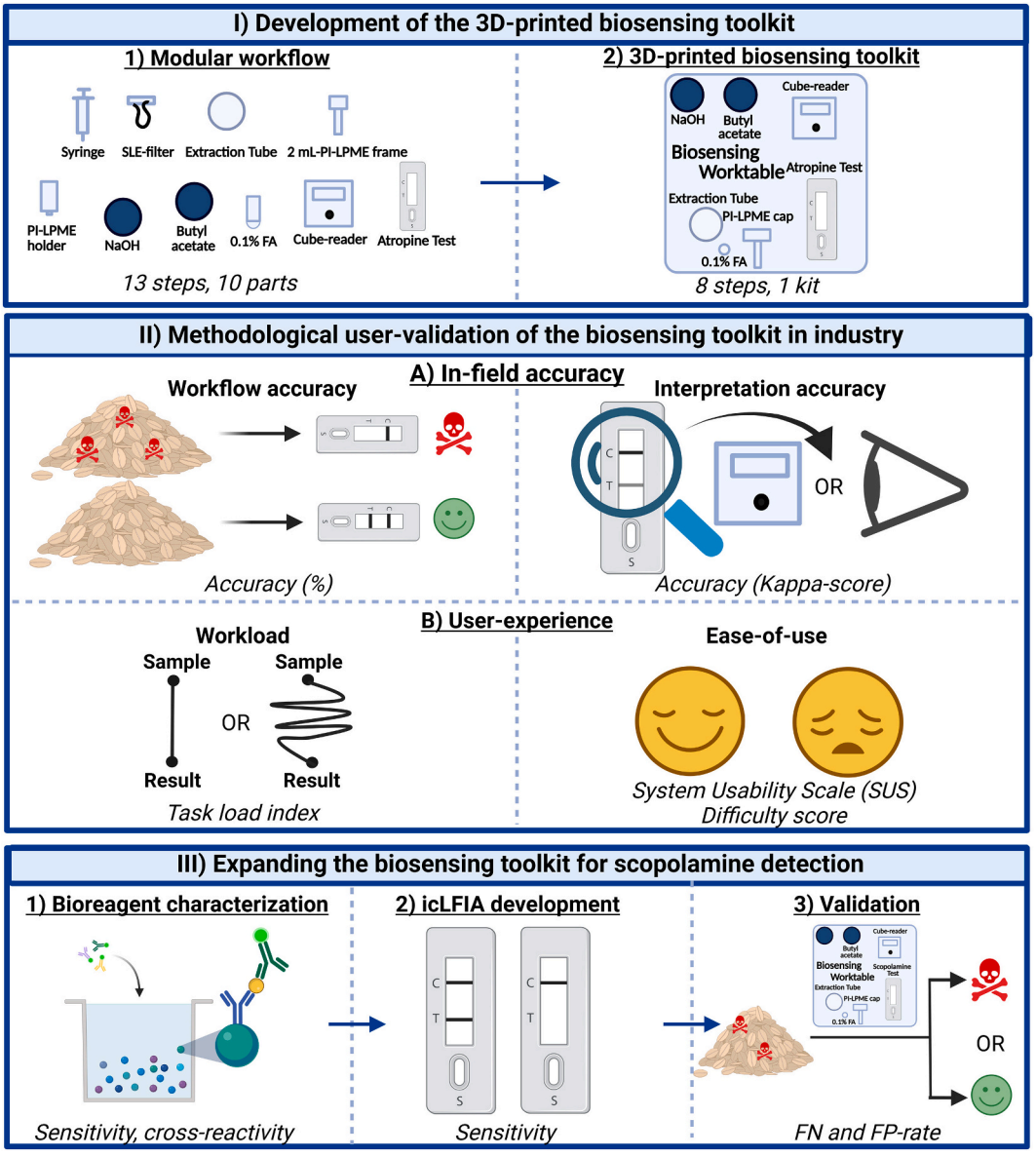

Fig. 1. Schematic overview of (**I**) the development of the 3D-printed biosensing toolkit, (**II**) methodological user-validation in industry, and (**III**) expansion of the biosensing toolkit for scopolamine detection (created with biorender.com).

contaminated with tropane alkaloids (de Nijs et al., 2023). In addition, buckwheat is experiencing a renewed commercial interest due to its valuable nutritional composition (Cirlini et al., 2018). Subsequently, all buckwheat cereals were analyzed with a validated LC-MS/MS method to verify these did not contain tropane alkaloids above the limit of detection (0.3 μg kg^{-1}) (Veršilovskis et al., 2020). Then, two grams of blank samples were precisely weighed in the extraction tube and then spiked with different concentrations of tropane alkaloid in 200 μL of ACN (0, 50, 100, or 1000 ng mL^{-1}) to achieve contamination levels of 0, 5, 10, 100 μg kg^{-1}. Subsequently, the buckwheat cereals were dried for at least 24 h and each cereal aliquot was thoroughly mixed prior to further use. For information on how to obtain the required number of 2 g replicate samples from bulk lots of milled buckwheat cereals for analysis with the biosensing toolkit in accordance with EU Regulations 2023/2782 and 2023/2783 (see SI, Protocol S1).

2.3. Instrumental setups

2.3.1. 3D-design, development, and 3D-printing of sample preparation and detection modules

Computer-aided design software SOLIDWORKS Education Edition 2021–2022 (SOLIDWORKS Corp; Waltham, USA) was used for designing the 3D-printable parts and converting them to printable .STL files. All 3D-printed components that come in contact with butyl acetate (e.g. the paper-immoblized liquid phase microextraction (PI-LPME) cap and holder) were printed with a stereolithography (SLA) printer Form3 (FormLabs; Summerville, USA) at a layer resolution of 100 μM using proprietary clear resin V5, because it has a high compatibility with butyl acetate (Formlabs, 2024). After printing, the resin parts were washed with isopropyl alcohol:H_2O (70/30, *v*/v) for 15 min, dried under a nitrogen flow, and subsequently cured using 405 nm light for 1 h at RT with a Form Cure V1 (FormLabs; Summerville, USA). The components were then ready for use. A fused deposition modeling (FDM) Original Prusa i3 MK3S+ printer (Prusa Research; Praque, Czech Republic) was used to print the biosensing worktable and the icLFIA cassette (see SI,

Table S1 for printer settings). After printing, the components were directly ready for use. As both during the SLA and FDM printing standard settings were used, the 3D-printed components of the biosensing toolkit can be easily printed using a wide-variety of different 3D-printers (Prabhakar et al., 2021; Saifuddin et al., 2022). All .3mf Files can be found in the supplementary information (SI, see Print-files).

2.3.2. Microsphere-based immunoassay

A microsphere-based immunoassay was used to characterize the sensitivity and cross-reactivity of the antibody raised against scopolamine. For this, a MAGPIX planar array analyzer (Luminex; Austin, USA) equipped with xPONENT 4.3 software (Luminex; Austin, USA) was used for read-out of the fluorescence of the microspheres. The acquisition volume was set at 50 µL. GraphPad Prism version 10 (Domatics; Boston, USA) was used for data processing and for five-parameter logistic curve fitting.

2.4. Development of the biosensing toolkit

The biosensing toolkit was constructed from readily available laboratory consumables and 3D-printed components. For recording the intensity of the test line (T-line) and control line (C-line), i.e. grey colour intensity on the icLFIA, a digital reader was used (Cubereader; Chembio Diagnostics GmbH; Berlin, Germany). After development of the 3D-printed biosensing toolkit, it was used to analyze 5 blank and 5 contaminated buckwheat cereal samples containing 10 µg kg^{-1} atropine, following SI, Protocol S2. In addition, a pilot study was conducted with five first-time users with laboratory experience similar to the QC-employees of Barilla, to evaluate usability and test performance by first-time users at regulatory levels. This panel analyzed in total 10× blank, 10× 5 µg kg^{-1}, and 10× 10 µg kg^{-1} atropine containing buckwheat cereal samples. The experimental set-up was blind as each participant started by first analyzing one buckwheat cereal sample contaminated with 10 µg kg^{-1}, without knowing this sample was contaminated. Subsequently, each participant analyzed 5 samples (2× blank, 2× 5 µg kg^{-1}, and 1× 5 µg kg^{-1}) simultaneously, without knowing which sample was blank or contaminated. The experimental workflow was similar as during the user-validation in industry, and can therefore be found in Section 2.5.2.

2.5. Methodological user-validation in industry

2.5.1. User-validation: Study-design

The user-validation of the biosensing toolkit was completed over 14 days (13-Jan-2025 to 24-Jan-2025) at multiple QC-laboratories of Barilla G.R. F.lli S.p.A company distributed throughout Italy. Participants were recruited during two (online) information sessions held on October 5 and November 10, 2024 with QC and research and development (R&D) managers from various production plants, with the aim of recruiting as many participants as possible. In total, 60 Barilla employees expressed interest in participating in the user-validation (see SI, Fig. S1 for a flow diagram showing the participation inclusion, allocation, and distribution of the samples). Only employees with no prior experience with operating icLFIAs - apart for personal medical use (e.g. SARS-CoV-2 or pregnancy test) - were eligible to participate in the user-validation. These participants were then distributed in an expert (n = 31) and non-expert (n = 29) group based on their laboratory experience. Those with regular laboratory experience, either current or past, were classified as experts, whereas participants with no or very limited laboratory experience were classified as non-experts. Detailed information about the participants' job description, level of education, and age distribution, can be found in the SI, Table S2. For both groups, sample distribution was performed in a blinded and randomized manner, as participants selected their own samples for analysis without prior knowledge of whether the sample was negative or positive. Informed consent from all participants was obtained prior to commencing the study.

2.5.2. User-validation: Experiments

The user-validation was conducted in two phases: expert testing, in which employees with laboratory experience (QC and R&D employees) tested the complete biosensing workflow, and non-expert testing, in which employees without laboratory experience interpreted the icLFIA (see Fig. 2).

During the expert testing, the in-field accuracy and user-experience of the participants operating the biosensing toolkit was assessed. Once the participants arrived at the test location, they were instructed to watch an instructional video (see SI, Video). Subsequently, they received a falcon tube with 2 g of blank (sample A) or spiked buckwheat cereals with 100 µg kg^{-1} atropine (sample B), the biosensing toolkit, and an icon-based instruction sheet (see SI, Fig. S2). At that point, the participants could start to analyze their buckwheat cereal samples using the biosensing toolkit. During testing, the participants were allowed to ask any questions to the test supervisors in case they could not solve this with the icon-based instruction sheet. However, the test-supervisors noted all the questions asked. For analysis, the participants interpreted their icLFIA results, first visually and then with a digital reader. As reference, the test supervisors subsequently also measured the same icLFIAs using the digital reader. At the end of the assessment, the participants were asked to fill out a questionnaire (see SI, Questionnaire S1).

During the non-expert testing, the participants received a positive, negative, or invalid icLFIA and an icon-based instruction sheet on how to interpret these icLFIAs (see SI, Fig. S3). Subsequently, the participants interpreted the icLFIA (first visually and then with a digital reader) and filled out their result in the questionnaire (see SI, Questionnaire S2). In case a participant forgot to fill in a question in the questionnaire, this question was discarded.

2.5.3. User-validation: Data evaluation

During the expert testing, the biosensing toolkit was evaluated on in-field accuracy and user-experience. In-field accuracy was defined as "the accuracy and completeness with which specified end-users can achieve specified goals in particular environments" (Jing et al., 2022). In the present study, in-field accuracy was further divided into two components: workflow accuracy and interpretation accuracy. Workflow accuracy was evaluated by checking the ability of the expert participants to obtain a correct icLFIA result when analyzing blank or contaminated buckwheat samples. Interpretation accuracy was evaluated by checking the ability of the expert participant to correctly interpret the icLFIA results. Interpretation accuracy was also assessed during the non-expert testing.

For workflow accuracy, after analysis of the buckwheat with the biosensing toolkit, the test supervisor also measured the intensities of the test-line (T-line) and control-line (C-line) with the digital reader. The software of the digital reader was used to obtain grey scale intensity values for each line, across the length of the icLFIA. The grey scale intensities were normalized by dividing the T-line by the C-line intensity, to obtain the T/C-ratio (Mahmoudi et al., 2020). In the previously published laboratory validation of the icLFIA-based modular workflow for atropine detection, a T/C-ratio of 0.69 was established as the cut-off value between blank and contaminated buckwheat cereal samples with 5 µg kg^{-1} atropine (estimated FN-rate of 5% and estimated FP-rate of 2.71%) (Lemmink et al., 2024). Therefore, the workflow accuracy was quantified, following:

$$\text{Workflow accuracy} = \frac{(TP + TN)}{N} * 100\% \quad (1)$$

where TP = true positive: total number of contaminated buckwheat cereal samples that obtained a T/C-ratio $\leq$ 0.69 (i.e. correctly identified as suspect), TN = true negative: total number of negative buckwheat

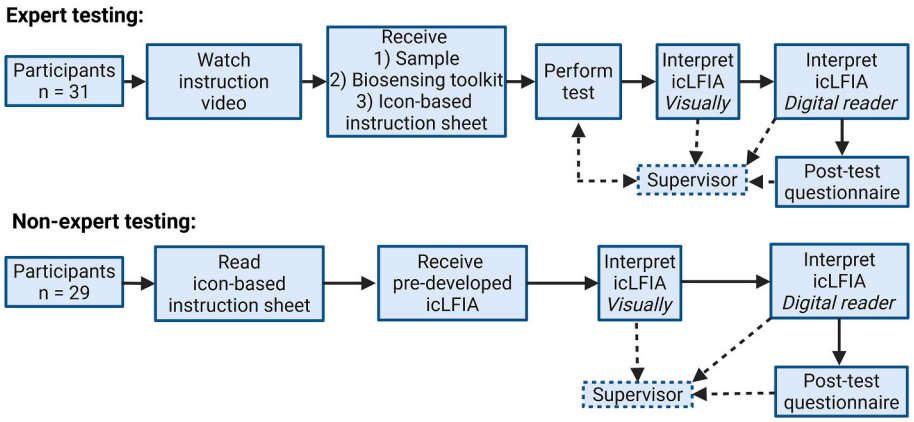

Fig. 2. Schematic overview of the steps taken by the participants during the expert and non-expert testing of the user-validation (created with biorender.com). All steps taken by the participants are indicated with regular arrows, interactions between the participant and the test supervisor are indicated with dashed arrows. If the dashed arrow is one-sided this indicates that the experimental/questionnaire results of the participants are collected by the test supervisor. In case the dashed arrow is two-sided this indicates (the possibility for) questions of the participant to the test supervisor.

cereal samples that obtained a T/C-ratio > 0.69 (i.e. correctly identified as negative), and N = total number of blank and contaminated buckwheat cereal samples.

In addition, the obtained T/C-ratios were grouped by day to assess inter-day repeatability using a one-way ANOVA. Furthermore, stability was evaluated by comparing the T/C-ratios obtained for blank buckwheat cereal samples analyzed during the user-validation with those obtained during prior in-house testing approximately one month earlier using a *t*-test.

The interpretation accuracy was evaluated with a Kappa-score, in which the agreement between the interpretation of the expert and non-expert participants and the interpretation by the test supervisors with the digital reader (ground truth) were assessed (Atchison et al., 2021; Figueroa et al., 2018; Kurth et al., 2016; Landis & Koch, 1977; Lee et al., 2007), following:

$$\text{Kappa score} = \frac{p_o - p_e}{1 - p_e} \quad (2)$$

where p_o = the observed agreement between the participants and the test supervisors, and p_e = the expected agreement between the participants and the test supervisors as a result of chance (see SI, Protocol S3 for the exact calculation of p_e and p_o).

The Kappa-scores were interpreted following: < 0 = poor agreement, 0.00–0.20 = slight agreement, 0.21–0.40 = fair agreement, 0.41–0.60 = moderate agreement, 0.61–0.80 = substantial agreement, and > 0.8 = almost perfect agreement (Landis & Koch, 1977).

After the sample handling and interpretation was performed, the in-field accuracy was calculated following Eq. 1, only now using the interpretation results of the end-users.

User-experience was also divided into two components: ease-of-use and workload. Ease-of-use referred to how easily expert participants could operate the biosensing toolkit, while the perceived workload described the resources (e.g. mental and physical) required to do so (Jing et al., 2022). The ease-of-use of the biosensing toolkit was evaluated using a system usability scale (SUS, see SI, Questionnaire S1, section Q5) (Brooke, 1996; Jing et al., 2022). Following previous user-experience studies, to obtain more detailed information about the difficulty of the steps within the workflow, the participants were asked to answer 21 questions (3 open questions and 18 questions on a five-point Likert scale, see SI, Questionnaire S1, section Q1-Q4) (Jing et al., 2022; Soares et al., 2023). The 18 questions on a five-point Likert scale were evaluated using a difficulty score following:

$$\text{Difficulty score} = \sum_{i=1}^{5} \left(n_i \times 2^{5-i}\right) - n_t \quad (3)$$

Where n_i = the number of expert participants who selected response option *i*, based on how easy they found a step; $i = 1$: strongly disagree (i.e. not easy at all), $i = 2$: disagree, $i = 3$: neutral, $i = 4$: agree, $i = 5$: strongly agree (i.e., very easy), n_t = total number of participants.

This scoring method assigns higher weights to responses indicating greater perceived difficulty. Thus, the difficulty score reflects both the frequency and the severity of experienced difficulty as reported by expert participants.

The perceived workload was estimated using the raw NASA's task load index (TLX) score (see Questionnaire S1, section Q6). The raw TLX (i.e. without weighting the contribution of each factor in a predefined manner) was used as it has a high correlation with the weighted TLX, but is simpler and more efficient to apply (Jing et al., 2022).

A priori acceptance criteria for the 3D-printed biosensing toolkit before the user-validation were defined as: (i) an in-field accuracy (workflow accuracy + interpretation accuracy) with a false-negative rate ≤ 5%, in line with EU Regulation 2023/2783; (ii) a SUS-score of ≥80/100, indicating good to best imaginable usability and being consistent with industrial practice (Lewis, 2018); and (iii) a raw TLX-score of ≤30/100, reflecting a medium to low perceived workload (Grier, 2015).

2.6. Biosensing toolkit expansion with a scopolamine-specific icLFIA: Development and validation

2.6.1. Bioreagent characterization

Based on the feedback gathered during the user-validation, the biosensing toolkit for atropine detection was expanded for scopolamine by the development and a laboratory validation of a scopolamine-specific icLFIA. For this reason, first, an antibody raised against scopolamine and synthesized scopolamine-BSA conjugate were evaluated for their sensitivity and specificity for seven different, but structurally-related tropane alkaloids in an indirect competitive microsphere-based immunoassay. For the synthesis protocol of the scopolamine-BSA conjugate see SI, Fig. S4. The protocol for the indirect competitive microsphere-based immunoassay measurements has been described in the SI (see Protocol S4) (Zou et al., 2022). The median fluorescence intensity (MFI) of approximately 100 microspheres was measured with the MAGPIX™ system. After five-parameter logistic curve fitting, half-maximum inhibitory concentration (IC_{50}) for each of the seven different tropane alkaloids were estimated with GraphPad Prism version 10 (Domatics: Boston, USA). The specificity was expressed in terms of cross-reactivity (CR):

$$CR = \frac{IC_{50}[\text{target TA}]}{IC_{50}[\text{competing TA}]} \times 100\% \quad (4)$$

Where CR = cross reactivity (%), IC_{50}[target TA] = half-maximum inhibitory concentration of the target tropane alkaloid (ng mL^{-1}), and IC_{50}[competitor TA] = half-maximum inhibitory concentration of another tropane alkaloid (ng mL^{-1}) (Wang et al., 2021).

2.6.2. Indirect competitive lateral flow immunoassay development

After the sensitivity and specificity of the scopolamine-specific antibody and scopolamine-BSA conjugate were determined, an icLFIA was developed, by optimizing the type of NC-membrane, RB-composition, drying buffer composition, and primary scopolamine-specific antibody, secondary goat anti-rabbit carbon-labelled antibody, scopolamine-BSA conjugate, and donkey anti-goat antibody concentrations. For a schematic overview of the final icLFIA, see SI (Fig. S5). Scopolamine calibration standards of 0, 0.1, 0.5, 1, 5, 10, and 30 ng mL^{-1} in RB were prepared to test the sensitivity of the developed icLFIA in a 3D-printed icLFIA cassette. The icLFIAs were wetted with 100 µL of calibration standard solution and allowed to develop for 15 min. After 15 min, the intensities of the test-line (T-line) and control-line (C-line) were measured with a digital reader.

2.6.3. Laboratory validation

When the scopolamine-specific icLFIA was developed and integrated in the biosensing toolkit, it was validated in the lab for the detection of scopolamine in milled buckwheat cereals by measuring 24 blank and contaminated buckwheat samples spiked at 0.5× maximum level (5 µg kg^{-1}) and maximum level (10 µg kg^{-1}), distributed over three consecutive days. Each sample was analyzed following protocol S2 and the instruction video (see SI) (Lemmink et al., 2024). After analyzing the samples with the immunoassay, a cut-off value with a 5%-FN rate (β = 0.05) between blank and contaminated buckwheat cereal samples with 5 µg kg^{-1} scopolamine was determined, following EU regulation 2023/2783 (see SI, Protocol S5) (European Commission, 2023).

3. Results and discussion

3.1. 3D-printed biosensing toolkit development

To reduce the number of samples that need to be transported to high-end laboratories for LC-MS/MS analysis, assays enabling cost-effective screening at the point-of-need can be implemented (Lemmink et al., 2025). Such screening assays for tropane alkaloids often rely on indirect competitive lateral flow immunoassays (icLFIAs), owing to the superior selectivity achieved through the use of antibodies (Lemmink, Straub, et al., 2024). However, icLFIAs already developed for tropane alkaloid detection have three major drawbacks: (i) they focus on relatively simple (viscous) liquid matrices (e.g. saliva, urine, or honey), (ii) have LODs above the European regulatory limits, or (iii) require a workflow with extensive laboratory-oriented sample preparation (Garrido et al., 2022; Mol et al., 2008; Mulder et al., 2014; Wang et al., 2023; Xu et al., 2022). Only recently, we reported the first modular workflow for atropine detection in buckwheat cereals at regulatory levels (Lemmink et al., 2024). To enhance user-friendliness, this modular workflow is now upgraded into a fully integrated 3D-printed toolkit (see Fig. 3A for an overview, and SI, Video for a demonstration of usage of the biosensing toolkit). Although the main steps during operation of the biosensing toolkit are the same as in the modular workflow, the new PI-LPME cap (see Fig. 3B) and the new PI-LPME holder (see Fig. 3C) have been designed to enhance operational simplicity. For example, the PI-LPME cap allows the PI-LPME to be directly performed inside the SLE-tube, removing the necessity of transferring a part of the SLE-extract to an 2-mL Eppendorf tube. In addition, the new PI-LPME holder is directly connected to the icLFIA cassette via a plastic stopcock valve. This allows the running buffer, in which atropine is eluted, to flow directly onto the icLFIA in the 3D-printed cassette instead of manually removing a stopper. A cost and greenness assessment of the 3D-printed biosensing toolkit can be found in the SI (Table S3 and Fig. S6).

To evaluate the performance of the new biosensing toolkit and to assess whether the cut-off value (T/C ratio = 0.69) established during a previous laboratory validation of the modular workflow remained applicable, blank and contaminated buckwheat cereal samples containing 10 µg kg^{-1} atropine (the regulatory limit) were analyzed (see SI, Fig. S7) (Lemmink et al., 2024). Using this threshold, all samples were correctly classified. Therefore, this cut-off was also used during the user-validation. In addition, during a pilot study at regulatory levels, five first-time users could clearly discriminate blank and contaminated buckwheat cereal samples containing 5 or 10 µg kg^{-1} atropine (see SI, Fig. S8).

3.2. User-validation in industry

After the development of the biosensing toolkit, it was methodologically evaluated in a user-validation study at Barilla company (see SI, Fig. S9 for photos taken during the user-validation). During this user-validation, the in-field accuracy and user-experience were assessed. The in-field accuracy was divided into two components: workflow accuracy (Section 3.2.1) and interpretation accuracy (Section 3.2.2), and user-experience was divided into: perceived workload (Section: 3.2.3)

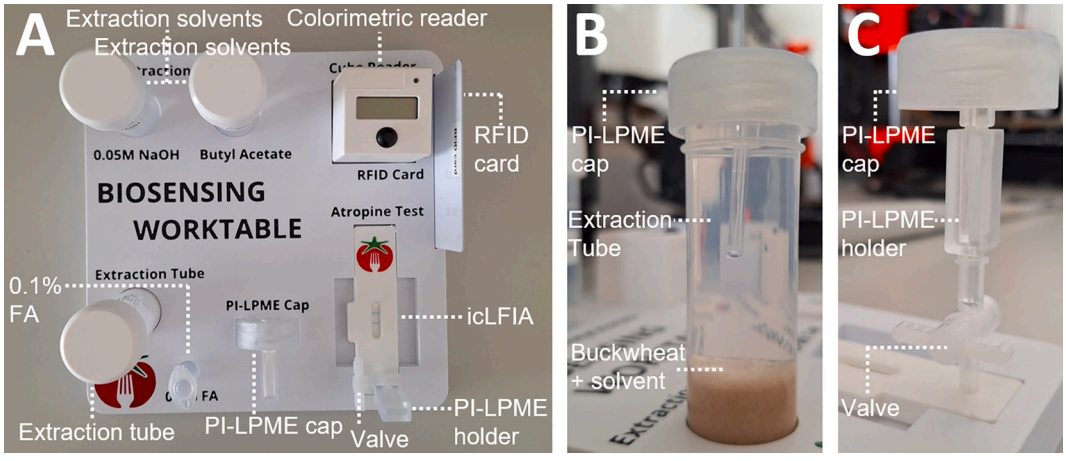

Fig. 3. Overview of the 3D-printed biosensing toolkit with, (**A**) top view of the complete 3D-printed biosensing toolkit, (**B**) side view of the PI-LPME cap screwed on the extraction tube for a PI-LPME, and (**C**) side view of the PI-LPME cap being inserted in the PI-LPME holder which is connected to a plastic valve.

and ease-of-use (Section 3.2.4).

3.2.1. Workflow accuracy

To assess workflow accuracy, all icLFIA strips resulting from the analysis of the blank and contaminated buckwheat cereal samples by the expert participants were presented to a test supervisors, who subsequently recorded the T/C ratios (see Fig. 4). In this manner, the user-induced uncertainty originating from the readout-step was excluded, allowing it to be studied separately for the assessment of the read-out accuracy (see Section 3.2.2). When applying the previously established T/C threshold of 0.69 (Lemmink et al., 2024), all blank samples had a T/C-ratio > 0.69, while all contaminated samples had a T/C-ratio ≤ 0.69, ensuring a 100% classification accuracy ($n = 31$, see Fig. 4). Despite this 100% classification accuracy, 3 out of 31 participants noted errors in there sample handling that potentially affected analytical performance. Specifically, one participant indicated that the cereals were not fully pre-wetted with NaOH, potentially resulting in a lower extraction recovery. Another participant reported that the PI-LPME paper was partially displaced from the PI-LPME frame during wetting, while a third participant experienced both issues. To prevent such sample-handling steps from occurring in the future, iterative improvements are further discussed in Section 3.2.4 (Ease of use and end-user feedback for iterative improvement). In addition, to prevent unnoticed sample-handling errors from leading to false-negative results, it is recommended to always include a positive reference sample contaminated at or near the regulatory limit, when implementing the biosensing toolkit.

In terms of repeatability, the biosensing toolkit had a high inter-day repeatability, as there were no significant differences in the icLFIA results over different days of the user-validation ($p > 0.05$). In addition, no significant differences were found between the T/C-ratios obtained after analyzing blank samples during the user-validation and those measured approximately one-month earlier ($p > 0.05$, see SI, Fig. S7), which indicates good stability under storage conditions during transport and at the point-of-need.

3.2.2. Interpretation accuracy

Interpretation accuracy was defined as the ability of the end-user to interpret the corresponding icLFIA results both visually and with a digital reader. Digital read-out requires approximately 20 s (see SI, Video) while the time needed for visual interpretation can vary substantially depending on the perceived difficulty of the icLFIA result and the end-user. Given the interpretation results, the in-field accuracy of the expert end-users (i.e. participants with laboratory experience) was 97% with visual read-out and 100% with automated read-out (see Fig. 5). With this in-field accuracy, the first a priori criteria – (i) FN-rate $< 5\%$ - has been accomplished, which indicates that with the biosensing toolkit its possible for the intended end-users to distinguish between blank and contaminated buckwheat cereal samples.

To assess our first hypothesis – (i) when analyzing blank or highly contaminated buckwheat samples, errors will arise more frequently from complex sample handling than from interpretation of the icLFIA result – the expert end-user workflow accuracy obtained was compared to their interpretation accuracy. For these end-users, the workflow accuracy was 100% (see Section 3.2.1) and the interpretation was in almost perfect agreement with the test supervisor when interpreting the icLFIA visually (Kappa-score = 0.94, 95CI = 0.81–1.0) or with a digital reader (Kappa-score = 1.00, see Fig. 5A). Therefore, hypothesis (i) was falsified, which indicates that with the 3D-printed tools the complex sample handling required for the atropine-test was substantially simplified, leading to better performance than anticipated.

For our second hypothesis – automated icLFIA read-out will be more accurate then visual read-out - the results for the non-experts supported this hypothesis. Visual interpretation was only in moderate agreement (Kappa-score: 0.46, 95CI = 0.21–0.70) with the test supervisor, while the interpretation of the non-expert end-users significantly improved to almost perfect agreement (Kappa-score: 0.89, 95CI = 0.74–1.0), when using a digital reader (see Fig. 5B). These results indicate that especially for the non-expert end-user, interpretation by a digital reader is required. The invalid results from the non-expert group involved icLFIAs where the C-line was missing (intentional, during production). When the expert end-users operated the 3D-printed biosensing toolkit, these intentionally invalid icLFIA were not used and also not accidentally obtained. However, if such invalid tests had occurred, the digital reader is programmed to immediately detect the absence of the C-line and therefore would have classified the icLFIA as invalid.

For our third hypothesis – (iii) expert end-users will interpret icLFIA results more accurately than non-expert end-users - when interpreting icLFIAs visually this hypothesis was supported, whereas when digital icLFIA-readout was used this hypothesis was falsified. Given that the non-expert end-users using digital read-out were able to interpret icLFIAs correctly, it may be feasible to train these regular employees (e.g. factory workers) to perform straightforward food safety tests in the future.

Overall, the interpretation results indicate that especially for the non-expert end-user, interpretation by a digital reader is required. This result is in line with prior user-validations with sandwich-format LFIAs, where the researchers reported that interpretation of a sandwich-format LFIA is often challenging especially when only a weak-test line is present (Jing et al., 2022). It is important to note that with a sandwich-format LFIA, both strong and weak test lines indicate a positive result. In contrast, in a competitive-format LFIA, a strong test line indicates a

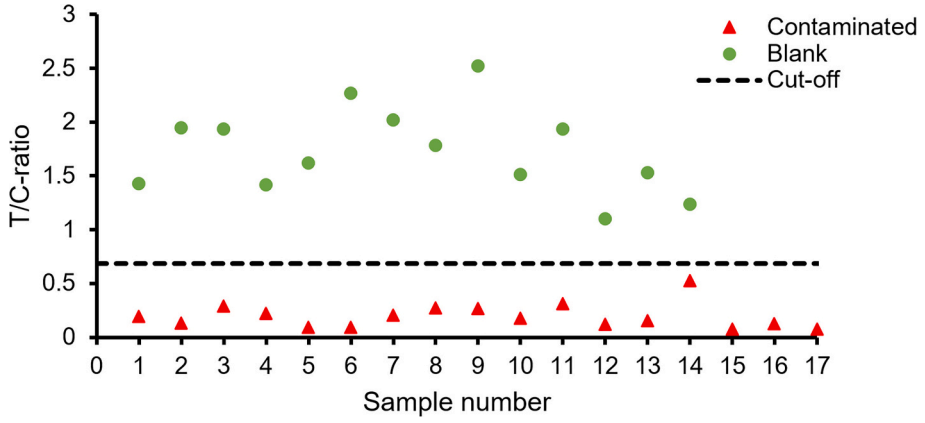

Fig. 4. T/C-ratios of the icLFIA's measured by the test supervisors using the digital reader, after 31 R&D/QC-employers analyzed 14 blank and 17 spiked buckwheat samples with 100 μg kg^{-1}: T/C-ratio obtained for the blank buckwheat (green circles), T/C-ratio obtained for the contaminated buckwheat (red triangles), and cut-off (dashed black line). (For interpretation of the references to colour in this figure legend, the reader is referred to the web version of this article.)

A) Expert end-user

		Visual interpretation		
		Positive	Negative	Invalid
Ground truth	Positive (17)	16	1	0
	Negative (14)	0	14	0
	Invalid (0)	0	0	0

		Digital reader		
		Positive	Negative	Invalid
Ground truth	Positive (17)	17	0	0
	Negative (14)	0	14	0
	Invalid (0)	0	0	0

B) Non-expert end-user

		Visual interpretation		
		Positive	Negative	Invalid
Ground truth	Positive (12)	11	0	1
	Negative (12)	9	3	0
	Invalid (5)	0	0	5

		Digital reader		
		Positive	Negative	Invalid
Ground truth	Positive (12)	11	0	1
	Negative (12)	0	11	1
	Invalid (5)	0	0	5

Fig. 5. Comparison of interpretation of icLFIA results by (**A**) expert end-users and (**B**) non-expert end-users, using either visual inspection or a digital reader. Cells indicating correct identifications are highlighted in green, while those indicating incorrect identifications are highlighted in red. (For interpretation of the references to colour in this figure legend, the reader is referred to the web version of this article.)

negative sample, while a weak test line suggests a positive sample – potentially causing mis-classifications. As a result, the misinterpretation of a weak test line in competitive-format LFIAs may have more serious implications than in a sandwich-format LFIA, further highlighting the need for digital read-out.

3.2.3. *Workload*

Workload was defined as the amount of resources used to achieve the required goals, and was estimated by using a normalized NASA's TLX (Jing et al., 2022). Several studies have found the TLX to be a valid measure to assess a subjective workload, consisting of: mental demand, physical demand, temporal demand, performance, effort, and frustration (Jing et al., 2022; Rubio et al., 2004). It has been used widely to measure workload in a broad range of applications in e.g. technology or healthcare domains (Hart, 2006; Jing et al., 2022; Weinger et al., 2000; Yurko et al., 2010). Raw TLX (without weighting the contribution of each factor in a predefined manner) has a high correlation with the weighted TLX, but is simpler and more efficient to apply (Jing et al., 2022). Therefore, in this study no weighting was applied for the TLX-score. The results of the normalized TLX-scores are 31 (±6) for mental demand, 21 (±6) for physical demand, 15 (±5) for performance, 24 (±5) for temporal load, and 18 (±3) for frustration (see SI, Fig. S10). With an average TLX score of 24 (±8), the biosensing toolkit is classified to have only a medium subjective workload (see SI, Table S4 for a distribution of the TLX score per subgroup) (Grier, 2015). Furthermore, with this TLX, the second a priori acceptance criteria – (ii) TLX-score $\leq$ 30 - was successfully accomplished.

Given this low workload, in the future, it is likely possible to let quality control personnel operate multiple biosensing toolkits at the same time.

Moreover, compared to a previously reported AbC-19 LFIA (LFIA to check if a person has IgG antibodies against SARS-CoV-2), which analyzed a drop of blood from the finger, our test obtained a comparable TLX score of 24 (±8) vs 27 (±19) (Jing et al., 2022). It must be stated that our envisioned end-users were predominantly QC-personnel with laboratory experience, where in case of the AbC-19 LFIA it were regular citizens who frequently have no laboratory experience. On the other hand, in our method substantial sample pretreatment was preformed – a step missing in many rapid (bio)sensing tools – yet this did not appear to increase the perceived workload.

3.2.4. *Ease-of-use and end-user feedback for iterative improvement*

The ease-of-use of the biosensing toolkit was assessed using a SUS. A SUS score of 88 (±8, n = 31) out of 100 was obtained, indicating an excellent (B) rating (see SI, Table S4 for a distribution of the SUS per subgroup) (Lewis, 2018). With this SUS the third a priori acceptance (SUS > 80) was successfully accomplished, and above the generally acknowledged cut-off for industrial application (Bangor et al., 2009). To further evaluate the ease-of-use of the individual steps within the workflow, participants responded to 3 open-questions (see SI, Table S5–7), and 18 questions on a five-point Likert scale, which were converted into a difficulty score (see Fig. 6). The newly developed difficulty score (observed range: 1–21) was used in addition to the traditional mean Likert score (observed range: 4.5–5.0), as it amplifies differences in perceived difficulty between workflow steps, thereby facilitating identification of steps that were perceived as more difficult by some participants. In addition, workflow steps that obtained a similar mean Likert score, could be differentiated using the new difficulty score (see SI, Fig. S11A). For example, the 3 workflow steps that obtained a mean-Likert score of 4.7 obtained difficulty scores ranging between 12 and 18, due to differences in the individual participant responses (see SI, Fig. S11B).

In the first section of the workflow (SLE), only one step – "shaking the extraction tube manually" (Question 1e, difficulty score = 21) – received a difficulty score above the average of 9. In the corresponding open-ended question, 4 out of 31 participants mentioned difficulty in determining the appropriate shaking speed (see SI, Table S5: Response 1–4). For this reason, 2 out of 31 participants noted that their cereal samples were not fully pre-wetted with NaOH solution before adding the butyl acetate (See SI, Table S5: Response 2 and 3). To address these challenges, the instructions in the icon-based instruction sheet have been improved by modifying the phrase "Shake for five seconds" to "Shake vigorously for five seconds, to fully wet the cereals" (see SI, Fig. S12; step 2, for the adjusted version of the icon-based instruction sheet).

In the second section of the workflow (PI-LPME), three steps received a difficulty score above the average. Two of these steps – "wetting the PI-LPME paper with 10 μL 0.1% FA" (difficulty score = 15, Question Q2c) and "inserting the PI-LPME cap into the icLFIA holder" (difficulty score = 18, Question Q2e) – were related. In the open-ended responses, 2 out of 31 participants reported that while pipetting, the PI-LPME paper was partially pushed out of the PI-LPME frame (see SI, Table S6: Response 1 and 2). As a result, inserting the frame with the displaced paper into the icLFIA holder became a challenge. A potential improvement could be to implement a slightly modified 3D-printed design with a fixed paper to prevent this issue. The other step that obtained a difficulty score above the average was – "identifying the 2 mL Eppendorf tube containing 0.1% FA" (difficulty score = 15, Question Q2b). Four participants mistakenly pipetted butyl acetate from the SLE section onto the PI-LPME paper instead of formic acid. However, all of them recognized their mistake themselves directly, when in the subsequent step they should place the

Question	Response: (5 = strongly agree, 1 = strongly disagree) 5 4 3 2 1	Likert score	Difficulty score
Q1e: The extraction tube was easily shaken manually		4.5	21
Q2e: The PI-LPME cap was easily inserted in the icLFIA holder	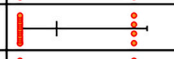	4.7	18
Q3c: The tap on the PI-LPME holder was easily opened	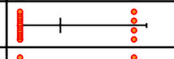	4.6	17
Q3f: The measurement on the colorimetric reader was easily started	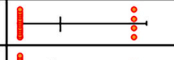	4.6	17
Q2b: The 2 mL Eppendorf tube with 0.1% FA was easily identified	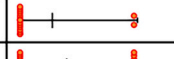	4.7	15
Q2c: The paper inside the PI-LPME cap was easily wetted with 10 µL 0.1% FA	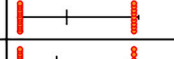	4.6	15
Q3e: The colorimetric reader was easily connected to the icLFIA	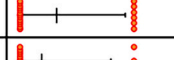	4.7	12
Q3g: The output of the colorimetric reader was easily interpreted	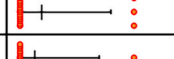	4.8	10
Q3a: The colorimetric reader was easily identified		4.9	8
Q3d: The atropine-test was easily interpreted visually	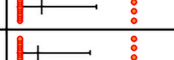	4.8	7
Q2a: The PI-LPME cap was easily identified	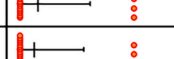	4.8	6
Q1d: The 4 mL 0.05M NaOH solution was easily added to the extraction tube	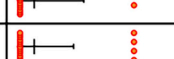	4.9	5
Q1a: The tube with 4 mL 0.05M NaOH solution was easily identified	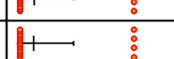	4.9	4
Q1b: The tube with 20 mL butyl acetate was easily identified	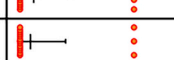	4.9	4
Q3b: The RFID card was easily identified	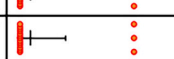	4.9	3
Q1f: The 20 mL butyl acetate was easily added to the extraction tube	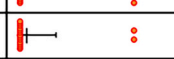	4.9	3
Q1c: The extraction tube with 2 gram of cereals was easily identified	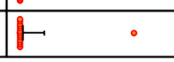	4.9	2
Q2d: The PI-LPME cap was easily screwed upon the extraction tube	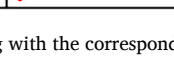	5.0	1

Fig. 6. Participant responses to the questionnaire items, along with the corresponding mean Likert scores, and difficulty scores (see Materials and Methods, Eq. 3). Individual responses are marked with red circles, the vertical bar indicates the mean response, and the error bars represent the standard deviation ($n = 31$). (For interpretation of the references to colour in this figure legend, the reader is referred to the web version of this article.)

PI-LPME frame into the SLE-holder. After asking the test supervisors, they were provided with a new PI-LPME cap to repeat this step. In order to avoid this mistake in the future, the use of colour-coded labels on the tubes was suggested multiple times by the expert participants (See SI, Table S5: Response 5 and 6, and Table S6: Response 3). Notably, the four requests for a new PI-LPME cap were the only four questions asked to the supervisors during the user-validation. This indicates that the biosensing toolkit demonstrates high operational robustness, as it can be operated using only provided instruction material (instruction video and icon-based instruction sheet), and additional equipment was only required during 4 out of 31 operations. Although the use of an additional PI-LPME cap has resulted in a small amount of extra waste, participants independently recognized their mistake and requested a replacement. Thus, providing an additional cap did not result in an overestimation of field-performance. In real-world settings a QC-lab would have access to sufficient biosensing toolkit components to perform multiple tests. Consequently, operators would simply retrieve a replacement item from the available supply when needed, rather than requesting one.

In the final section of the workflow (icLFIA analysis), four steps received a difficulty score above the average (>9). The two most challenging steps – "opening the tap on the PI-LPME holder" (Question Q3c) and "starting the measurement using the digital reader" (Question Q3f) – both obtained a difficulty score of 17. For opening the tap, 2 participants noted difficulty in determining whether the tap was open or closed (see SI, Table S7: Response 1 and 2). A possible reason for this confusion is that the wicking of the solution through the icLFIA takes time, and the liquid front only becomes visible approximately one minute after opening the tap. Providing more clear instructions on the open and closed positions of the icLFIA tap can overcome this unclarity (see SI, Fig. S12; step 10, for an adjusted version of the instructions). In addition an evaluation of the development of the T/C-ratio when analyzing blank or contaminated buckwheat samples has been performed, and highlights the importance to only analyze the atropine-test 15 min after opening the tap (see Fig. S13). To make this more clear for the end-user the instructions in step 11 has been better specified (see SI, Fig. S12; step 11). For starting the measurement with the digital reader, currently, it requires two manual presses and one press with the RFID card, limiting current user-experience. The other two steps with difficulty scores >9 were "positioning the digital reader over the icLFIA" (difficulty score = 12, Question Q3e) and "interpreting the output of the digital reader" (difficulty score = 10, Question Q3g). If the digital reader was positioned incorrectly over the icLFIA, it generated an error response, ensuring that incorrect placement did not affect the identification process. For the interpretation of the output of the digital reader the results in Fig. 5A show that this did not affect the final identification as all the identifications were correct. To guide future operators of the 3D-printed biosensing toolkit in dealing with potential sample-handling errors and their consequences, a risk assessment has been integrated in the icon-based instruction sheet (see SI, Fig. S12). If any of these sample-handling errors are observed and the analysis result is negative, the analysis should be repeated.

One additional point raised during the industrial user-validation was that tropane alkaloids are regulated as the sum of atropine and scopolamine with a limit of 10 µg kg^{-1} in milled buckwheat cereals (EU regulation 2023/915). Reviewing all reported cases of tropane alkaloid contamination in buckwheat cereals within the European Union from 2010 to 2023, atropine was consistently the tropane alkaloid present at the highest concentration (de Nijs et al., 2023; Lemmink et al., 2024).

Therefore, if atropine levels are below 5 μg kg^{-1} it is likely that scopolamine levels are also below 5 μg kg^{-1}, meaning the legal limit is not exceeded. However, companies would likely prefer to be on the safe side and therefore screen their food commodities for both atropine and scopolamine. In response to this, a scopolamine-specific icLFIA was developed enabling scopolamine detection with the 3D-printed biosensing toolkit (see Section 3.3).

3.3. Expanding the biosensing toolkit with a scopolamine-specific icLFIA: Development and validation

3.3.1. Bioreagent characterization

In order to develop a scopolamine-specific icLFIA, first the sensitivity and specificity of the antibody raised against scopolamine were determined for seven different tropane alkaloids using an indirect competitive microsphere-based immunoassay (see SI, Fig. S14 and Table S8). The lowest IC50-value was obtained for scopolamine (0.22 ng mL^{-1}), followed by anisodine (1.38 ng mL^{-1}, CR = 15%) and aposcopolamine (6.68 ng mL^{-1}, CR = 3.4%). Based on these CR-values, the presence of anisodine at ~66 μg kg^{-1} or aposcopolamine at ~294 μg kg^{-1} in buckwheat would be expected to produce an assay response comparable to that of scopolamine at ~10 μg kg^{-1} (EU-regulatory limit). However, the risk of false positive results due to anisodine or aposcopolamine is low, as these compounds are typically present at substantially lower concentrations than atropine or scopolamine (de Nijs et al., 2023; Mulder et al., 2016). For example, in anoccurrence study in which 268 single component flours (including buckwheat) and 578 cereal-based products were analyzed, anisodine and aposcopolamine were only present above LOD in ≤1% of samples, compared to ≥5% for scopolamine and ≥ 10% for atropine (Mulder et al., 2016). Moreover, in the positive samples, average concentrations of anisodine and aposcopolamine were approximately tenfold lower than those of scopolamine and atropine.

3.3.2. icLFIA development

The scopolamine-specific antibody and in-house synthesized scopolamine-BSA conjugate were integrated in an icLFIA (see SI, Fig. S5), and its sensitivity for scopolamine was tested in running buffer. Here, an IC_{50}-value of 0.86 ng mL^{-1} (see SI, Fig. S15) was obtained, making its sensitivity comparable to previously reported icLFIAs for scopolamine detection (IC_{50}-values: 0.51–1.03 ng mL^{-1}) (Sun et al., 2024; Wang et al., 2023). For a comparison between the atropine-specific and scopolamine-specific icLFIA see SI (Table S9).

3.3.3. Laboratory validation of the 3D-printed biosensing toolkit with a scopolamine-specific icLFIA

Subsequently, the scopolamine-specific icLFIA was integrated in the 3D-printed biosensing toolkit, and validated by analyzing blank and contaminated buckwheat cereal samples spiked with scopolamine (see Fig. 7). A T/C-ratio of 0.70 was established as cut-off value between blank and contaminated buckwheat cereal samples with 5 μg kg^{-1} scopolamine (estimated FN-rate of 5% and estimated FP-rate of 1.6%). Therefore, our biosensing toolkit with the scopolamine-specific icLFIA can detect scopolamine at regulatory levels in buckwheat cereals and, together with the previously validated icLFIA for atropine, help companies to screen their food commodities for both atropine or scopolamine.

3.4. Outlook

Here, a 3D-printed biosensing toolkit that allows for either the detection of atropine or scopolamine in buckwheat cereals at regulatory levels is reported. During the user-validation in industry, the biosensing toolkit was well-received by end-users and – given that a digital reader is used – the in-field accuracy was good. Therefore, our biosensing toolkit represents a promising tool for food companies and food safety institutions to screen buckwheat cereals on the presence of atropine or scopolamine, especially considering that a rapid screening workflow is often more cost-effective than traditional LC-MS/MS workflows (Lattanzio et al., 2013). Further research will focus on expanding the biosensing toolkit workflow with other (potentially aptamer-based) LFAs for strictly regulated food contaminants in the field of natural toxins. Perhaps most importantly, the methodological user-validation underscores the importance of evaluating point-of-need tools for food safety screening in terms of their user-experience and in-field accuracy, ensuring a better understanding of their eventual performance in the field. This study thus provides a framework that can adopted more broadly for providing evidence for claims about ease-of-use and application potential at the point-of-need for innovative (bio)sensing approach in and beyond food safety.

Supplementary data to this article can be found online at https://doi.org/10.1016/j.foodchem.2026.148889. The supplementary material contains: Instruction video; 3D-print files; 3D-printer settings; biosensing-toolkit operation procedure; participant information; icon-based instruction sheet; questionnaire; immunoassay protocols; synthesis of conjugate; cost-assessment; AGREEprep assessment; photos of user-validation; responses to open questions; evaluation task load index score; comparison different lateral flow immunoassays; validation

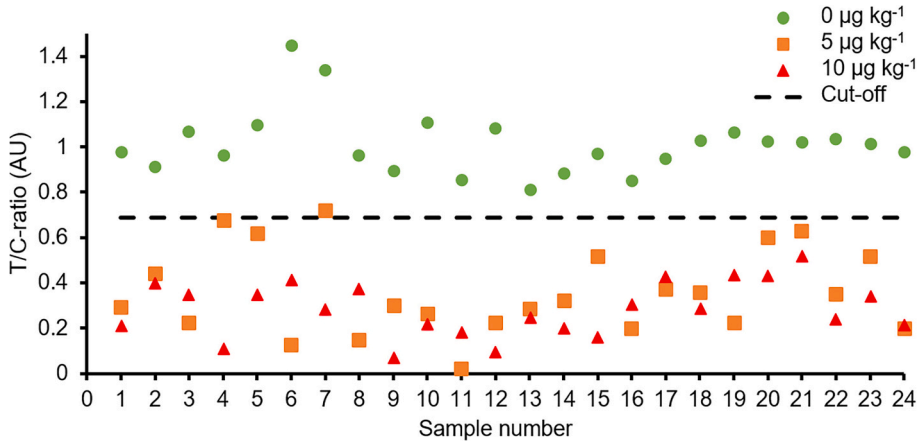

Fig. 7. T/C ratios of the icLFIA after analyzing 24 blank and spiked buckwheat samples at 5 μg kg^{-1} (0.5× maximum level) and 10 μg kg^{-1} (1.0× maximum level) scopolamine with the modular workflow: T/C ratio for the blank samples (green circles), 5 μg kg^{-1} samples (orange squares), or 10 μg kg^{-1} samples (red triangles), and cut-off with an estimated false negative rate (FN) of 5% (dashed black line). (For interpretation of the references to colour in this figure legend, the reader is referred to the web version of this article.)

results.

Declaration of AI-assisted technologies in the writing process

During preparation of this work the authors used ChatGPT to evaluate the readability of several sentences. After using this tool/service, the authors reviewed and edited the content as needed and take(s) full responsibility for the content of the publication.

CRediT authorship contribution statement

Ids B. Lemmink: Writing – original draft, Visualization, Validation, Project administration, Methodology, Investigation, Formal analysis, Data curation, Conceptualization. **Eleonora Rollo:** Writing – review & editing, Project administration, Methodology, Investigation, Formal analysis, Data curation. **Erik Beij:** Writing – review & editing, Methodology, Formal analysis. **Anne-Catherine Huet:** Writing – review & editing, Resources. **Toine F.H. Bovee:** Writing – review & editing, Supervision, Resources. **Michele Suman:** Writing – review & editing, Supervision, Resources, Project administration, Methodology, Funding acquisition, Conceptualization. **Gert IJ. Salentijn:** Writing – review & editing, Supervision, Resources, Project administration, Methodology, Funding acquisition, Conceptualization.

Declaration of competing interest

The authors declare that they have no known competing financial interests or personal relationships that could have appeared to influence the work reported in this paper.

Acknowledgments

The authors like to thank Prof. Dr. Han Zuilhof and Liza Portier for the useful discussions. This work (FoodSafeR) has received funding from the European Union's Horizon Europe research and innovation programme under grant agreement No. 101060698. This work was supported by the Dutch Ministry of Agriculture, Fisheries, Food Security and Nature through the Knowledge development program 'Healthy and safe food systems' (project KB-37-002-023).

Data availability

Data will be made available on request.

References

Atchison, C., Pristerà, P., Cooper, E., Papageorgiou, V., Redd, R., Piggin, M., … Ward, H. (2021). Usability and acceptability of home-based self-testing for severe acute respiratory syndrome coronavirus 2 (SARS-CoV-2) antibodies for population surveillance. *Clinical Infectious Diseases, 72*(9), 384–393. https://doi.org/10.1093/cid/ciaa1178

Bangor, A., Kortum, P., & Miller, J. (2009). Determining what individual SUS scores mean: Adding an adjective rating scale. *Journal of Usability Studies, 4*, 114–123. https://doi.org/10.1145/238386.238459

Brooke, J. (1996). SUS—A quick and dirty usability scale. *Usability Evaluation in Industry., 189*(194), 4–7. https://doi.org/10.1201/9781498710411-35

Cirlini, M., Demuth, T. M., Biancardi, A., Rychlik, M., Dall'Asta, C., & Bruni, R. (2018). Are tropane alkaloids present in organic foods? Detection of scopolamine and atropine in organic buckwheat (Fagopyron esculentum L.) products by UHPLC–MS/MS. *Food Chemistry, 239*, 141–147. https://doi.org/10.1016/j.foodchem.2017.06.028

Dzuman, Z., Jonatova, P., Stranska-Zachariasova, M., Prusova, N., Brabenec, O., Novakova, A., … Hajslova, J. (2020). Development of a new LC-MS method for accurate and sensitive determination of 33 pyrrolizidine and 21 tropane alkaloids in plant-based food matrices. *Analytical and Bioanalytical Chemistry, 412*(26), 7155–7167. https://doi.org/10.1007/s00216-020-02848-6

European Commission. (2023). Regulation (EU) 2023/2783 laying down methods of sampling and analysis for the control of levels of plant toxins in food. https://eurlex.europa.eu/eli/reg_impl/2023/2783.

Figueroa, C., Johnson, C., Ford, N., Sands, A., Dalal, S., Meurant, R., … Baggaley, R. (2018). Reliability of HIV rapid diagnostic tests for self-testing compared with testing by Health-care workers: A systematic review and Meta-analysis. *Lancet HIV, 5*(6), e277–e290. https://doi.org/10.1016/S2352-3018(18)30044-4

Formlabs. Clear Resin V5 Technical Data Sheet. 2024, 1–2, https://media.formlabs.com/m/5fd5e7daf14600 58/original/ -ENUS-Clear-Resin-V5-TDS.pdf.

Garrido, E., Climent, E., Marcos, M. D., Sancenón, F., Rurack, K., & Martínez-Máñez, R. (2022). Lateral flow assay for simultaneous scopolamine and "cannibal drug" detection based on receptor-gated mesoporous nanoparticles. *Nanoscale, 14*, 13505–13513. https://doi.org/10.1039/d2nr03325a

Geballa-Koukoula, A., Ross, G. M. S., Bosman, A. J., Zhao, Y., Zhou, H., Nielen, M. W. F., … Salentijn, G. IJ. (2023). Best practices and current implementation of emerging smartphone-based (bio)sensors – Part 2: Development, validation, and social impact. *TrAC Trends in Analytical Chemistry, 163*, Article 116986. https://doi.org/10.1016/j.trac.2023.116986

Gonçalves, C., Cubero-Leon, E., & Stroka, J. (2020). Determination of tropane alkaloids in cereals, tea and herbal infusions: Exploiting proficiency testing data as a basis to derive interlaboratory performance characteristics of an improved LC-MS/MS method. *Food Chemistry, 331*, Article 127260. https://doi.org/10.1016/j.foodchem.2020.127260

Grassi, P. A., Gracia, M. E., & Fenton, J. L. (2017). *Digital Identity Guidelines*. NIST. https://doi.org/10.6028/NIST.SP.800-63-3

Gravador, R. S., Haughey, S., Meneely, J., Greer, B., Nugent, A., Daniel, C. S., & Elliott, C. (2024). Reports of tropane alkaloid poisonings and analytical techniques for their determination in food crops and products from 2013 to 2023. *Comprehensive Reviews in Food Science and Food Safety, 23*. https://doi.org/10.1111/1541-4337.70047

Grier, R. A. (2015). How high is high? A meta-analysis of NASA-TLX global workload scores. *Proc. Hum. Factors Ergon. Soc., 2015*(59), 1727–1731. https://doi.org/10.1177/1541931215591373

Grym, K., Niela-Vilén, H., Ekholm, E., Hamari, L., Azimi, I., Rahmani, A., … Axelin, A. (2019). Feasibility of smart wristbands for continuous monitoring during pregnancy and one month after birth. *BMC Pregnancy and Childbirth, 19*(1). https://doi.org/10.1186/s12884-019-2187-9

Hart, S. G. (2006). NASA-task load index (NASA-TLX); 20 years later. *Proceedings of the Human Factors and Ergonomics Society Annual Meeting, 50*(9), 904–908. https://doi.org/10.1177/154193120605000909

Jing, M., Bond, R., Robertson, L. J., Moore, J., Kowalczyk, A., Price, R., … Moore, T. (2022). User experience of home-based AbC-19 SARS-CoV-2 antibody rapid lateral flow immunoassay test. *Scientific Reports, 12*(1). https://doi.org/10.1038/s41598-022-05097-y

Kurth, A. E., Cleland, C. M., Chhun, N., Sidle, J. E., Were, E., Naanyu, V., … Siika, A. M. (2016). Accuracy and acceptability of Oral fluid HIV self-testing in a general adult population in Kenya. *AIDS and Behavior, 20*(4), 870–879. https://doi.org/10.1007/s10461-015-1213-9

Landis, J. R., & Koch, G. G. (1977). The measurement of observer agreement for categorical data. *Biometrics, 33*(1), 159–174. https://doi.org/10.2307/2529310

Lattanzio, V. M. T., Von Holst, C., & Visconti, A. (2013). Experimental Design for in-House Validation of a screening immunoassay kit: The case of a multiplex dipstick for *fusarium* mycotoxins in cereals. *Analytical and Bioanalytical Chemistry, 405*(24), 7773–7782. https://doi.org/10.1007/s00216-013-6922-1

Lee, V. J., Choon Tan, S., Earnest, A., Suet Seong, P., Hee Tan, H., & Sin Leo, Y. (2007). User acceptability and feasibility of self-testing with HIV rapid tests. *JAIDS J. Acquir. Immune Defic. Syndr., 45*, 449–453. https://doi.org/10.1097/QAI.0b013e318095a3f3

Lemmink, I. B., Bosma, S. J., Bovee, T. F. H., Zuilhof, H., & Salentijn, G. IJ. (2025). Paper-immobilized liquid-phase microextraction for direct paper spray mass spectrometry and immuno-detection of atropine in baby food, buckwheat cereals, and edible oils at regulatory levels. *Analytica Chimica Acta, 1349*. https://doi.org/10.1016/j.aca.2025.343823

Lemmink, I. B., Straub, L. V., Bovee, T. F. H., Mulder, P., Zuilhof, H., Salentijn, G. IJ., & Righetti, L. (2024). Recent advances and challenges in the analysis of natural toxins. *Advances in Food and Nutrition Research, 110*, 67–144. https://doi.org/10.1016/bs.afnr.2024.05.001

Lemmink, I. B., Willemsen, L., Beij, E., Bovee, T. F. H., Zuilhof, H., & Salentijn, G. IJ. (2024). Modular point-of-need tropane alkaloid detection at regulatory levels: Combining solid–liquid extraction from buckwheat with a paper-immobilized liquid-phase microextraction and immuno-detection in interconnectable 3D-printed devices. *Analytical Chemistry, 96*, 16462–16468. https://doi.org/10.1021/acs.analchem.4c04811

Lewis, J. R. (2018). The system usability scale: Past, present, and future. *Int. J. Comput. Interact., 34*, 577–590. https://doi.org/10.1080/10447318.2018.1455307

Mabey, D., Peeling, R. W., Ustianowski, A., & Perkins, M. D. (2004). Diagnostics for the developing world. *Nature Reviews. Microbiology, 2*(3), 231–240. https://doi.org/10.1038/nrmicro841

Mahmoudi, T., de la Guardia, M., & Baradaran, B. (2020). Lateral flow assays towards point-of-care Cancer detection: A review of current Progress and future trends. *TrAC Trends in Analytical Chemistry, 125*, Article 115842. https://doi.org/10.1016/j.trac.2020.115842

Marín-Sáez, J., Romero-González, R., & Frenich, A. G. (2019). Reliable determination of tropane alkaloids in cereal based baby foods coupling on-line SPE to mass spectrometry avoiding chromatographic step. *Food Chemistry, 275*, 746–753. https://doi.org/10.1016/j.foodchem.2018.09.137

Mol, H. G. J., Plaza-Bolaños, P., Zomer, P., De Rijk, T. C., Stolker, A. A. M., & Mulder, P. P. J. (2008). Toward a generic extraction method for simultaneous determination of pesticides, mycotoxins, plant toxins, and veterinary drugs in feed and food matrixes. *Analytical Chemistry, 80*, 9450–9459. https://doi.org/10.1021/ac801557f

Mulder, P. P. J., de Nijs, M., Castellari, M., Hortos, M., MacDonald, S., Crews, C., … Stranska, M. (2016). Occurrence of tropane alkaloids in food. *EFSA Supporting Publications*, 13. https://doi.org/10.2903/sp.efsa.2016.en-1140

Mulder, P. P. J., von Holst, C., Nivarlet, N., & van Egmond, H. P. (2014). Intra- and inter-laboratory validation of a dipstick immunoassay for the detection of tropane alkaloids hyoscyamine and scopolamine in animal feed. *Food Additives & Contaminants, Part A: Chemistry, Analysis, Control, Exposure & Risk Assessment, 31*(7), 1165–1176. https://doi.org/10.1080/19440049.2014.914249

Ng, O. T., Chow, A. L., Lee, V. J., Chen, M. I. C., Win, M. K., Tan, H. H., … Leo, Y. S. (2012). Accuracy and user-acceptability of HIV self-testing using an Oral fluid-based HIV rapid test. *PLoS One, 7*(9). https://doi.org/10.1371/journal.pone.0045168

de Nijs, M., Crews, C., Dorgelo, F., MacDonald, S., & Mulder, P. P. J. (2023). Emerging issues on tropane alkaloid contamination of food in Europe. *Toxins, 15*, 98. https://doi.org/10.3390/toxins15020098

Prabhakar, M. M., Saravanan, A. K., Lenin, A. H., Mayandi, K., & Ramalingam, P. S. (2021). A short review on 3D printing methods, process parameters and materials. *Materials Today Proceedings, 45*, 6108–6114. https://doi.org/10.1016/j.matpr.2020.10.225

Rausch, A.-K., Brockmeyer, R., & Schwerdtle, T. (2021). Development, validation, and application of a multi-method for the determination of mycotoxins, plant growth regulators, tropane alkaloids, and pesticides in cereals by two-dimensional liquid chromatography tandem mass spectrometry. *Analytical and Bioanalytical Chemistry*. https://doi.org/10.1007/s00216-021-03239-1

Rockström, J., Edenhofer, O., Gaertner, J., & DeClerck, F. (2020). Planet-proofing the global food system. *Nature Food, 1*, 3–5. https://doi.org/10.1038/s43016-019-0010-4

Ross, G. M. S., Zhao, Y., Bosman, A. J., Geballa-Koukoula, A., Zhou, H., Elliott, C. T., … Salentijn, G. IJ. (2023). Best practices and current implementation of emerging smartphone-based (bio)sensors – Part 1: Data handling and ethics. *TrAC Trends in Analytical Chemistry, 162*, Article 116863. https://doi.org/10.1016/j.trac.2022.116863

Rubio, S., Díaz, E., Martín, J., & Puente, J. M. (2004). Evaluation of subjective mental workload: A comparison of SWAT, NASA-TLX, and workload profile methods. *Applied Psychology, 53*(1), 61–86. https://doi.org/10.1111/j.1464-0597.2004.00161.x

Rusu, C., Rusu, V., Roncagliolo, S., & González, C. (2015). Usability and user experience: What should we care about? *Int. J. Inf. Technol. Syst. Approach, 8*(2), 1–12. https://doi.org/10.4018/IJITSA.2015070101

Saifuddin, K. K., Joshi, K., & Deshmukh, S. (2022). A comprehensive review on the effect of printing parameters on mechanical properties of FDM-printed parts. *Materials Today Proceedings, 50*, 2119–2212. https://doi.org/10.1016/j.matpr.2021.09.433

Soares, D. C., Filho, L. C. F., Souza dos Reis, H., Rodrigues, Y. C., Freitas, F. B., de Oliveira Souza, C., … Bazzo, M. L. (2023). Assessment of the accuracy, usability and acceptability of a rapid test for the simultaneous diagnosis of syphilis and HIV infection in a real-life scenario in the Amazon region, Brazil. *Diagnostics (Basel), 13*(4), Article 810. https://doi.org/10.3390/diagnostics13040810

Sun, B., Wang, C., Wang, Z., Liang, J., Han, K., Zhang, S., … Jiang, H. (2024). Strategy for accurate detection of six tropane alkaloids in honey using lateral flow immunosensors. *Sensors, 24*(22). https://doi.org/10.3390/s24227265

Veršilovskis, A., Mulder, P. P. J., Pereboom-de Fauw, D. P. K. H., de Stoppelaar, J., & de Nijs, M. (2020). Simultaneous quantification of ergot and tropane alkaloids in bread in the Netherlands by LC-MS/MS. *Food Additives & Contaminants, Part B: Surveillance, 13*(3), 215–223. https://doi.org/10.1080/19393210.2020.1771777

Wang, Z., Ma, Q., Zheng, P., Xie, S., Yao, K., Zhang, J., & Jiang, H. (2023). Generation of broad-spectrum recombinant antibody and construction of colorimetric immunoassay for tropane alkaloids: Recognition mechanism and application. *Journal of Hazardous Materials, 459*, Article 132247. https://doi.org/10.1016/j.jhazmat.2023.132247

Wang, Z., Zheng, P., Wang, J., He, S., Ren, Z., Zhang, Y., … Jiang, H. (2021). Indirect competitive enzyme-linked immunosorbent assay based on a broad-spectrum monoclonal antibody for tropane alkaloids detection in pig urine, pork and cereal flours. *Food Chemistry, 337*, Article 127617. https://doi.org/10.1016/j.foodchem.2020.127617

Weinger, M. B., Vredenburgh, A. G., Schumann, C. M., Macario, A., Williams, K. J., Kalsher, M. J., … Health, D. (2000). Quantitative description of the workload associated with airway management procedures. *Proceedings of the Human Factors and Ergonomics Society Annual Meeting, 44*(12), 621–624. https://doi.org/10.1016/S0952-8180(00)00152-5

Xu, X., Ge, W., Suryoprabowo, S., Guo, X., Zhu, J., Liu, L., Xu, C., & Kuang, H. (2022). Fluorescence-based immunochromatographic test strip for the detection of hyoscyamine. *Analyst, 147*, 293–302. https://doi.org/10.1039/d1an01973b

Yonel, Z., Kuningas, K., Sharma, P., Dutton, M., Jalal, Z., Cockwell, P., … Chapple, I. L. C. (2022). Concordance of three point of care testing devices with clinical chemistry laboratory standard assays and patient-reported outcomes of blood sampling methods. *BMC Medical Informatics and Decision Making, 22*(1). https://doi.org/10.1186/s12911-022-01999-z

Young, N., Achieng, F., Desai, M., Phillips-Howard, P., Hill, J., Aol, G., … Taegtmeyer, M. (2019). Integrated point-of-care testing (POCT) for HIV, syphilis, malaria and anaemia at antenatal facilities in Western Kenya: A qualitative study exploring end-users' perspectives of appropriateness, acceptability and feasibility. *BMC Health Services Research, 19*(1). https://doi.org/10.1186/s12913-018-3844-9

Yurko, Y. Y., Scerbo, M. W., Prabhu, A. S., Acker, C. E., & Stefanidis, D. (2010). Higher mental workload is associated with poorer laparoscopic performance as measured by the NASA-TLX tool. *Simulation in Healthcare, 5*(5), 267–271. https://doi.org/10.1097/SIH.0b013e3181e3f329

Zou, R., Guo, Y., Chen, Y., Zhao, Y., Zhao, L., Zhu, G., … Guo, Y. (2022). Computer-aided profiling of a unique broad-specific antibody and its application to an ultrasensitive Fluoroimmunoassay for five N-methyl carbamate pesticides. *Journal of Hazardous Materials, 426*, Article 127845. https://doi.org/10.1016/j.jhazmat.2021.127845

Zurek, M., Ingram, J., Bellamy, A. S., Goold, C., Lyon, C., Alexander, P., … Withers, P. J. A. (2022). Food system resilience: Concepts, issues, and challenges. *Annual Review of Environment and Resources*. https://doi.org/10.1146/annurev-environ-112320